

February, 1933

TECHNICAL NOTES

NATIONAL ADVISORY COMMITTEE FOR AERONAUTICS

No. 467

SIMPLIFIED AERODYNAMIC ANALYSIS OF THE
CYCLOGIRO ROTATING-WING SYSTEM

By John B. Wheatley
Langley Memorial Aeronautical Laboratory

~~FILE COPY~~

Washington
August 1933

NATIONAL ADVISORY COMMITTEE FOR AERONAUTICS

TECHNICAL NOTE NO. 467

SIMPLIFIED AERODYNAMIC ANALYSIS OF THE
CYCLOGIRO ROTATING-WING SYSTEM

By John B. Wheatley

SUMMARY

A simplified aerodynamic theory of the cyclogiro rotating wing is presented herein. In addition, examples have been calculated showing the effect on the rotor characteristics of varying the design parameters of the rotor. A performance prediction, on the basis of the theory here developed, is appended, showing the performance to be expected of a machine employing this system of sustentation.

The aerodynamic principles of the cyclogiro are sound; hovering flight, vertical climb, and a reasonable forward speed may be obtained with a normal expenditure of power. Autorotation in a gliding descent is available in the event of a power-plant failure.

INTRODUCTION

In carrying out a program of research on the general problem of rotating-wing systems, the National Advisory Committee for Aeronautics has undertaken a study of a power-driven rotor which, because of the cycloidal path described by the blades, is called the "cyclogiro." This rotor possesses promise in the field of hovering flight and vertical ascent, in addition to a reasonable speed in level flight.

For the purpose of investigating the basic merit of its aerodynamic principles, a simplified aerodynamic theory of the cyclogiro has been developed and is here presented. In its present form the theory must be considered as giving only qualitative results because of the simplifying assumptions found necessary in its derivation. For illustrative purposes, the theory has been applied to a rotor of assumed proportions, and the variation of the rotor characteristics with changes in the basic rotor parameters is shown in the form of horsepower-required curves.

DESCRIPTION

The cyclogiro rotating-wing system is shown in figure 1. The rotor consists of several blades rotating about a horizontal axis perpendicular to the direction of normal flight. The angle of the individual blades to the tangent of the circle of the blade's path is varied by a double-cam arrangement so designed that the periodic oscillation of the blades about their span axis may be changed both in amplitude and in phase angle (fig. 2). The net force on the rotor may thus be varied in magnitude and direction by movements of the cams.

THEORY

Referring to figure 2, velocities are those of the rotor with respect to the air and are positive upward and in the direction of normal flight, also in the direction of rotation and radially outward. Forces are positive in the same direction as velocities except that tangential forces are positive when resisting rotation. Blade angles are positive when the blade trailing edge is closer than the leading edge to the rotor axis.

Force and power coefficients will be based on the tip speed and projected area of the rotor, and are defined by the following equations:

$$C_Z = \frac{Z}{\rho \Omega^2 R^3 s} \quad (1)$$

where C_Z is the vertical force coefficient
 Z is the vertical force, lb.
 ρ is the air density, slugs per cu.ft.
 Ω is the rotor angular velocity, rad. per sec.
 R is the rotor radius, ft.
 s is the blade length parallel to the rotor axis, ft.

$$C_X = \frac{X}{\rho \Omega^2 R^3 s} \quad (2)$$

where C_X is the horizontal force coefficient
 X is the horizontal force, lb.

$$C_P = \frac{P}{\rho \Omega^3 R^4 s} \quad (3)$$

where C_P is the coefficient of power required
 P is the power required, ft.-lb. per sec.

It is assumed that the horizontal and vertical induced velocities v_x and v_z due to the generation of the forces X and Z are constant in magnitude throughout the rotor cylinder and, by analogy with propeller theory, are one-half the velocity increment imparted to the air in producing X and Z . Then if V is the translational velocity of the rotor and θ the flight-path angle referred to the horizontal forward, let

$$\mu \Omega R = V \cos \theta + v_x \quad (4)$$

$$\lambda \Omega R = V \sin \theta + v_z \quad (5)$$

and
$$V' = \Omega R (\lambda^2 + \mu^2)^{\frac{1}{2}} \quad (6)$$

where V' is the resultant velocity.

These velocities are diagrammed in figure 3.

It is further assumed that the area from which the induced velocity v_z is calculated is that of a circle of diameter s , in all cases where $V \cos \theta$ exceeds an arbitrary fraction - say 0.1 - of the tip speed; when $V \cos \theta < 0.1 \Omega R$, the area is assumed to be that of a rectangle of length s and width $2R$. This is equivalent to assuming that the rotor in forward flight acts like a monoplane in so far as the induced velocity v_z is concerned. The arbitrary speed $0.1 \Omega R$ has no great significance, since the extreme conditions of hovering flight and maximum forward speed are unaffected by it; its application to subsequent examples has been the termination of the horsepower-required curves before the velocity of translation reached zero. The use of the cross-sectional area $2Rs$ in hovering flight is equivalent to assuming that the rotor acts like a propeller. It is apparent that any error introduced by these assumptions will be quantitative, and will not affect the qualitative relations obtained in the subsequent expressions. The induced velocity v_x is assumed to be derived from the area $2Rs$ in all cases.

Then

$$v_z = \frac{2Z}{\rho V' \pi s^2} = \frac{2C_Z \Omega R^2}{\pi s (\lambda^2 + \mu^2)^{\frac{1}{2}}} \quad (7)$$

$$v_x = \frac{X}{4\rho V' R s} = \frac{C_X \Omega R}{4(\lambda^2 + \mu^2)^{\frac{1}{2}}} \quad (8)$$

Substituting the values for v_x and v_z in equations (4) and (5), they become

$$\lambda = \frac{V \sin \theta}{\Omega R} + \frac{2C_Z R}{\pi s (\lambda^2 + \mu^2)^{\frac{1}{2}}} \quad (9)$$

$$\mu = \frac{V \cos \theta}{\Omega R} + \frac{C_X}{4(\lambda^2 + \mu^2)^{\frac{1}{2}}} \quad (10)$$

Equations (9) and (10) may be used to solve for λ as a function of μ if it is assumed that $\frac{C_X}{4(\lambda^2 + \mu^2)^{\frac{1}{2}}}$ is negligible in comparison with $\frac{V \cos \theta}{\Omega R}$.

Dividing (9) by (10),

$$\frac{\lambda}{\mu} = \tan \theta + \frac{2C_Z R}{\pi \mu s (\lambda^2 + \mu^2)^{\frac{1}{2}}} \quad (11)$$

Let the tangential and radial velocities at the blade be designated U_t and U_r , respectively; let the resultant velocity be designated U , making the angle Φ with the tangent to the path circle. Then, referring to figure 4,

$$U_t = \Omega R - \mu \Omega R \sin \psi + \lambda \Omega R \cos \psi \quad (12)$$

where ψ is the blade-position angle referred to the horizontal forward

$$U_r = \mu \Omega R \cos \psi + \lambda \Omega R \sin \psi \quad (13)$$

$$U_r = U_t \tan \Phi \quad (14)$$

It will be assumed that Φ is small, so that $\tan \Phi = \Phi$. Then

$$U_t = U \quad (15)$$

$$U_r = U\Phi \quad (16)$$

The angle-of-attack variation of the blades is a sinusoidal function of ψ , and the instantaneous geometrical angle α can be expressed as

$$\alpha = \alpha_0 + \alpha_A \cos(\psi - \epsilon) \quad (17)$$

where α_0 is a constant angle setting with respect to the tangent of the blade-path circle

α_A is the amplitude of the varying angle

ϵ is the value of ψ at which the varying part of the angle is a positive maximum

The aerodynamic angle of attack α_T is equal to the difference between α and Φ . Then

$$\alpha_T = \alpha - \Phi = \alpha_0 - \Phi + \alpha_A \cos(\psi - \epsilon). \quad (18)$$

For the straight-line portion of the lift curve, the blade lift coefficient C_L may be written

$$C_L = a\alpha_T \quad (19)$$

where a is $\frac{dC_L}{d\alpha}$ for the blade profile, α being in radian measure. From this relation and equation (18), the instantaneous lift L and drag D of a blade may be written

$$\begin{aligned} L &= \frac{1}{2} \rho U^2 S a \alpha_T \\ D &= \frac{1}{2} \rho U^2 S C_{D_0} \end{aligned} \quad (20)$$

where S is the blade area

C_{D_0} is the average profile-drag coefficient of the blade section.

It is possible to express the profile drag of an airfoil section as a function of the minimum drag and the lift coefficient, but the inaccuracies incident to the assumptions regarding the inflow and the angle Φ do not justify such refinement. A value will be arbitrarily assigned to C_{D_0} , 50 percent greater than the minimum drag of the section, when applied in the equations, and will be assumed constant over the range of useful angles of attack.

Up to this point, equations have been derived for the forces on only one blade. In summing up the net force due to several blades, it will be assumed that interference between blades may be neglected.

The resolution of the L and D forces into X and Z components (see fig. 4) results in the equations

$$Z = \frac{b}{2\pi} \int_0^{2\pi} \left\{ L \sin(\psi - \Phi) - D \cos(\psi - \Phi) \right\} d\psi \quad (21)$$

$$X = \frac{b}{2\pi} \int_0^{2\pi} \left\{ L \cos(\psi - \Phi) + D \sin(\psi - \Phi) \right\} d\psi \quad (22)$$

where b is the number of blades.

Substituting from equations (12), (13), (15), (16), (18), and (20), integrating, and simplifying,

$$Z = \frac{1}{2} \rho \Omega^2 R^2 b S \left\{ a\alpha_A \sin \epsilon \left(\frac{1}{2} + \frac{1}{2} \mu^2 \right) - \frac{1}{2} a\alpha_A \mu \lambda \cos \epsilon \right. \\ \left. - \frac{3}{2} a\mu\alpha_0 - \frac{1}{2} a\lambda - \frac{3}{2} \lambda C_{D_0} \right\} \quad (23)$$

$$X = \frac{1}{2} \rho \Omega^2 R^2 b S \left\{ a\alpha_A \cos \epsilon \left(\frac{1}{2} + \frac{1}{2} \lambda^2 \right) - \frac{1}{2} a\alpha_A \mu \lambda \sin \epsilon \right. \\ \left. + \frac{3}{2} a\alpha_0 \lambda - \frac{1}{2} a\mu - \frac{3}{2} \mu C_{D_0} \right\} \quad (24)$$

For a blade of constant chord c , S is cs -- then the solidity σ of the rotor is defined as

$$\sigma = \frac{bc}{2\pi R} \quad (25)$$

$$C_Z = \pi \sigma \left\{ a \alpha_A \sin \epsilon \left(\frac{1}{2} + \frac{1}{2} \mu^2 \right) - \frac{1}{2} a \mu \lambda \alpha_A \cos \epsilon \right. \\ \left. - \frac{3}{2} a \mu \alpha_0 - \frac{1}{2} a \lambda - \frac{3}{2} \lambda C_{D_0} \right\} \quad (26)$$

$$C_X = \pi \sigma \left\{ a \alpha_A \cos \epsilon \left(\frac{1}{2} + \frac{1}{2} \lambda^2 \right) - \frac{1}{2} a \mu \lambda \alpha_A \sin \epsilon \right. \\ \left. + \frac{3}{2} a \lambda \alpha_0 - \frac{1}{2} a \mu - \frac{3}{2} \mu C_{D_0} \right\} \quad (27)$$

Energy is dissipated in the rotor only in the maintenance of the X and Z forces and in the losses arising from the blade profile drag. From equations (23) and (24) it is seen that X and Z involve the profile-drag coefficient; the power required for this part of the X and Z forces introduces the same factor twice into the power equation when the integral for the profile losses is set up. Adding a term to cancel out the profile-drag term in the X and Z forces, the equation determining the power required is written

$$P = \lambda \Omega R Z + \mu \Omega R X + \frac{b}{2\pi} \int_0^{2\pi} \frac{1}{2} \rho S U^2 \Omega R C_{D_0} d\psi + \\ \frac{3}{4} \rho \Omega^2 R^2 b S C_{D_0} (\mu^2 + \lambda^2) \quad (28)$$

Substituting from (11) and (14) and reducing to coefficient form,

$$C_P = \lambda C_Z + \mu C_X + \pi \sigma C_{D_0} (1 + 2\mu^2 + 2\lambda^2) \quad (29)$$

Equations (11), (26), (27), and (29) for λ , C_Z , C_X , and C_P , respectively, determine uniquely the condition of operation of the rotor when the physical dimensions, tip speed, air speed, and flight-path angle are chosen; that is, the power required to fly a given rotor at a given speed in a given direction can be calculated. Equation (29) may be used to show that the cyclogiro will autorotate in the event of a power-plant failure. From equations (26) and (27), it is seen that C_X and C_Z may be given any desired value by changing the control parameters α_A and ϵ . In a glide, the velocity factor λ becomes negative, as can be demonstrated by reference to equation (9).

The first term of equation (9) is negative when θ is negative; the second term is positive, but the relative magnitude of the two terms may be varied by increasing V , which increases the absolute magnitude of both μ and λ . This increase in V increases the magnitude of the negative first term, and decreases the magnitude of the positive second term, since all quantities but μ and λ are constant. The resultant expression for λ must then become negative as V increases if it was not negative at the start. Regardless, then, of the initial rate of rotation, equation (29) shows that the power coefficient C_P may be given a negative value, supplying an accelerating torque which may be used to attain any desired rate of rotation. Once rotation is attained, the values of α_A and ϵ may be adjusted so that the Z force equals the weight, the X force, the horizontal component of the drag, and the power coefficient C_P is equal to zero; the condition of steady flight at zero power, or autorotation, is then demonstrated.

DISCUSSION

For mathematical simplicity it has been assumed in the development of the theory that the induced velocities v_x and v_z are constant in magnitude throughout the rotor cylinder; this assumption introduces an error which probably varies in sign around the periphery of the rotor cylinder and which should have a relatively small effect upon the net forces and torque. The assumption that the tangent of Φ may be equated to Φ introduces an appreciable error when μ is large, but only where $\cos \psi$ is nearly unity; where the cosine ψ is large, the blade forces in normal flight are small, so that again the net forces and torque are reasonably accurate.

The area within which the air is influenced by the rotor forces has been assumed by analogy with monoplane airfoil theory and propeller theory. It is thought that the assumptions made regarding these areas are satisfactory; but errors introduced in so assuming are purely quantitative and do not affect any qualitative relations established in the theory.

The assumption stating that the interference is negligible introduces an error which probably varies directly with the number of blades and the rotor solidity. It is

felt, however, that correction may be made for the interference by multiplying by an empirical constant, which will be obtained from the analysis of experimental data. It is reasonable to assume that interference will introduce only a quantitative error in the net forces deduced by the equations developed in this paper.

On the basis of the preceding paragraphs, it can be stated that the equations developed for the net forces and torque of the cyclogiro rotor give satisfactory qualitative relations between the rotor characteristics and the parameters affecting them. It can then be stated that the aerodynamic principles of the cyclogiro are sound. It should be pointed out, however, that serious structural difficulties will attend the practical application of these principles. The control system will be necessarily complicated mechanically, and gyroscopic couples in the rotor will add complexities. The system possesses sufficient promise, nevertheless, to justify further work, and it is recommended that this theoretical study be supplemented by experiment.

EXAMPLES

Examples are attached showing the calculated effect of the basic rotor parameters on the power requirements of a sample rotor. The dimensions and physical characteristics of the sample rotor are given in table I.

In the consideration of the influence of the solidity and rotor loading on the rotor characteristics, it must be remembered that a blade should not be permitted to attain a stalling angle of attack in normal flight. With this point in view, the maximum instantaneous blade lift coefficient was calculated for an average set of conditions from equations (14) and (18), and compared with the average blade lift coefficient C_{L_A} . The coefficient C_{L_A} is based on the tip speed and blade area, and is found from the expression

$$C_{L_A} = \frac{2W}{bcs\Omega^2 R^2 \rho} = \frac{C_Z}{\pi\sigma} \quad (30)$$

It was found that the maximum instantaneous C_L was from four to five times C_{L_A} . This definitely limits the vari-

tion, one at a time, of the solidity, rotor loading, and tip speed, although C_{LA} may be held at a reasonable value by varying two or more parameters at the same time.

The effect of the aspect-ratio factor $\frac{s}{2R}$ is shown in figure 5 and needs little comment. In figure 6, a set of curves has been calculated in which the tip speed for any solidity has been varied to keep C_{LA} constant. It is seen that high solidities are advantageous, although the neglected interference effects may tend to neutralize the decrease in power requirement shown. Figure 7 presents the effect of changing $\frac{W}{2R_s}$ while keeping the weight constant. In this example also, C_{LA} has been held constant by changing the tip speed with rotor loading. The crossing of the power-required curves for the three loadings shown is due to the fact that the ratio between the induced and profile power requirements varies with the loading under the assumed conditions. Figure 8 shows the effect of varying C_{LA} by changing the solidity, the rotor loading, and the tip speed. The power required for the rotor defined in table I is shown for comparison. The increase in power required as C_{LA} is decreased is smallest, at low speed, when the rotor is enlarged; at high speed, the smallest increment is obtained by increasing the tip speed, while the largest increment is obtained by enlarging the rotor. The power required for hovering is shown in figures 9 and 10 as induced and parasitic power, the two factors being independent. Control characteristics are shown in figures 11 and 12, where the variation in the X and Z forces with ϵ and α_A , respectively, is presented.

The performance of a complete cyclogiro, the physical characteristics and dimensions of which are shown in table II, has been calculated and is presented in figures 13, 14, and 15. It will be noted that the assumed drag area of 20 square feet is conservative, even allowing for the necessary structural complications. It was considered useful to add to the performance calculation figure 16, in which the values of α_A and ϵ for the gliding phase of flight are shown as functions of air speed. Despite the conservative parasite drag assumed, the calculated performance is striking. Although the equations given do not apply at low forward speeds, the horsepower-required curves have been faired in to the point determined at zero forward speed.

CONCLUSIONS

The cyclogiro rotating-wing system is aerodynamically sound in principle.

Hovering flight, vertical ascent, and reasonable forward speed are obtained without the excessive expenditure of power in the cyclogiro.

The cyclogiro rotor will autorotate in a gliding descent.

Langley Memorial Aeronautical Laboratory,
National Advisory Committee for Aeronautics,
Langley Field, Va., July 14, 1933.

TABLE I

Assumed Basic Rotor Characteristics

Radius	$R = 6.0$ ft.
Span	$s = 24.0$ ft.
Blade chord	$c = 0.472$ ft.
Number of blades	$b = 4$
Solidity	$\sigma = 0.05$
Weight	$W = 1,440$ lb.
Rotor loading	$\frac{W}{2Rs} = 5.00$ lb. per sq. ft.
Pitch setting	$\alpha_0 = 0^\circ$
Tip speed	$\Omega R = 300$ ft. per sec.
Lift-curve slope	$a = 5.00$
Average profile-drag coefficient	$C_{D_0} = 0.015$
Parasite drag area	$A_D = 8.0$ sq. ft. = drag area propelled by rotor

TABLE II

Complete Cyclogiro Characteristics

Gross weight	=	3,000 lb.
Brake hp, available	=	300 hp.
Parasite drag area	=	20 sq. ft. (total)
Number of rotors	=	2
Loss in transmitting power to rotor	=	10 percent
Rotor:	σ	= 0.075
	ΩR	= 245 ft. per sec.
	R	= 6.00 ft.
	s	= 24.0 ft.
	$\frac{W}{2Rs}$	= 5.21 lb. per sq. ft.
	C_{D_0}	= 0.015
	α_0	= 0°
	a	= 5.00

Note: Rotors are assumed to act independently.

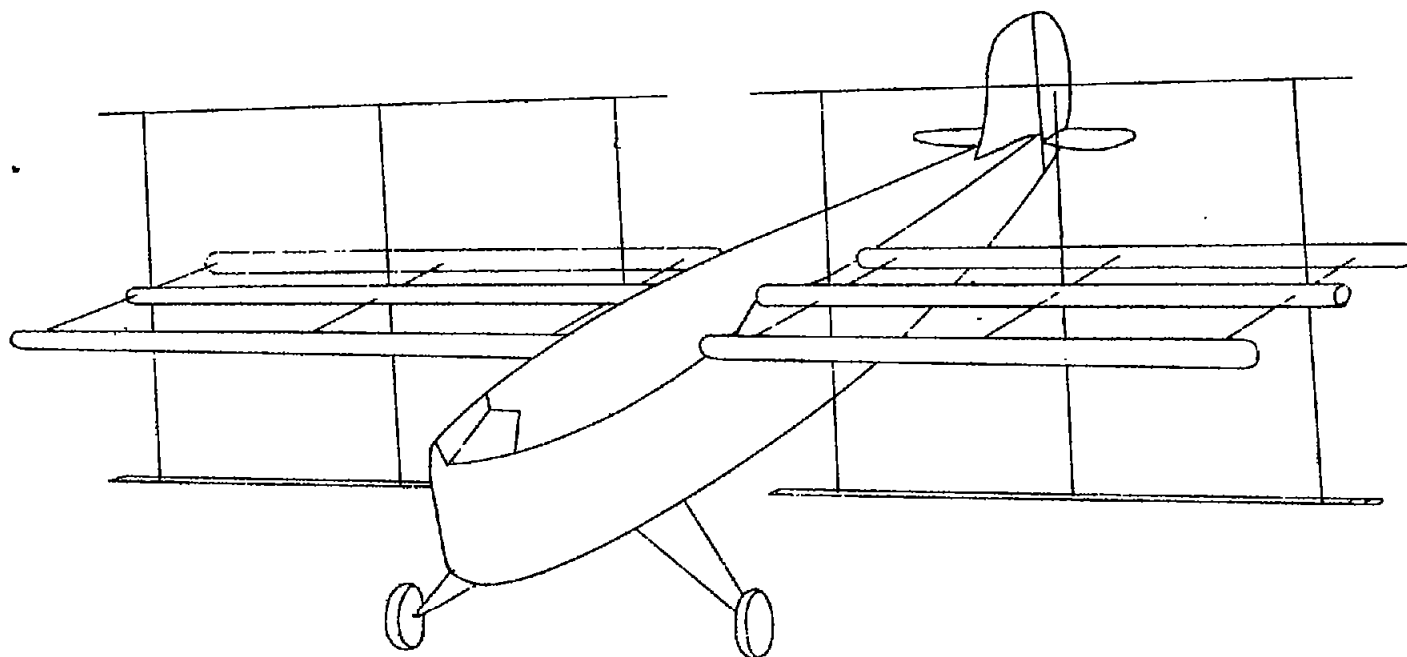


Figure 1.-The cyclogiro

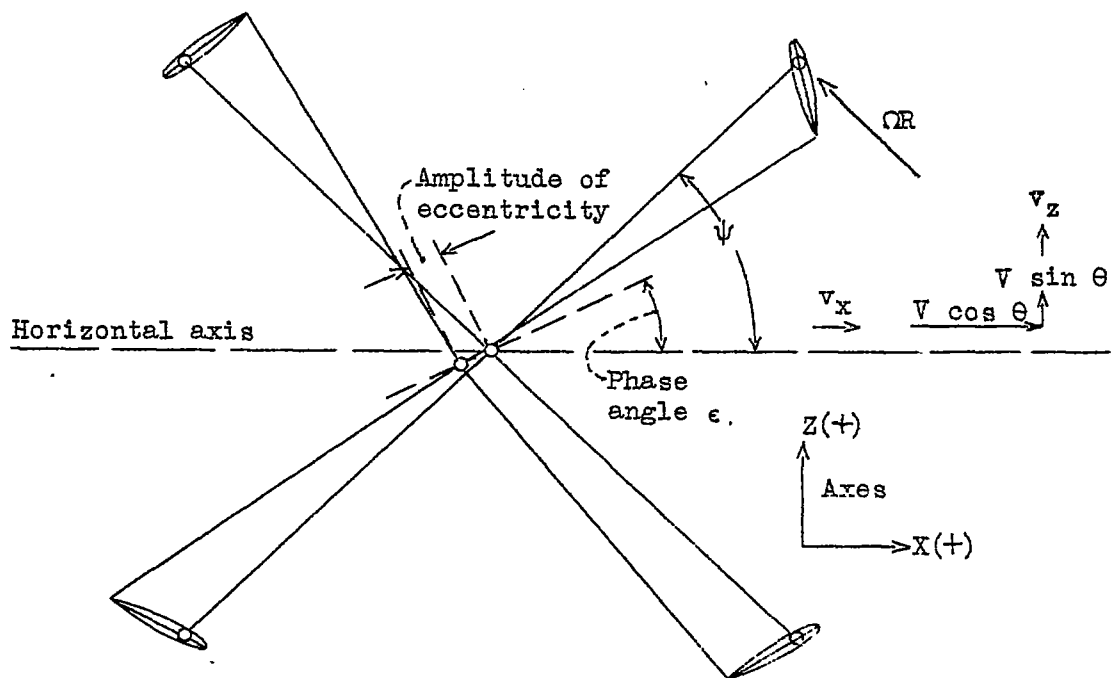


Figure 2.-Diagram of rotor system.

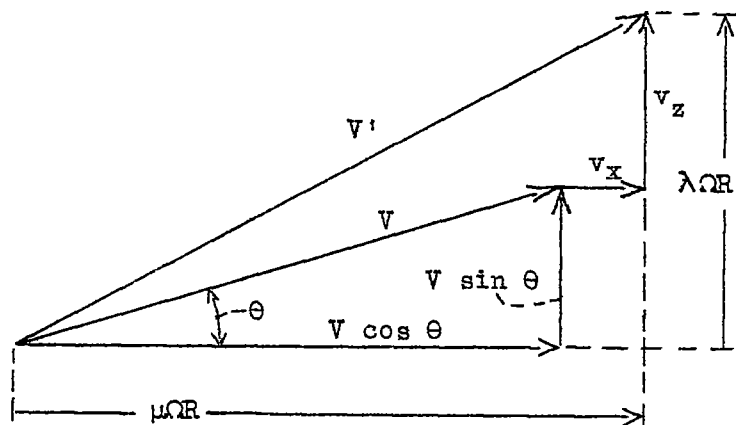


Figure 3.-Velocity diagram.

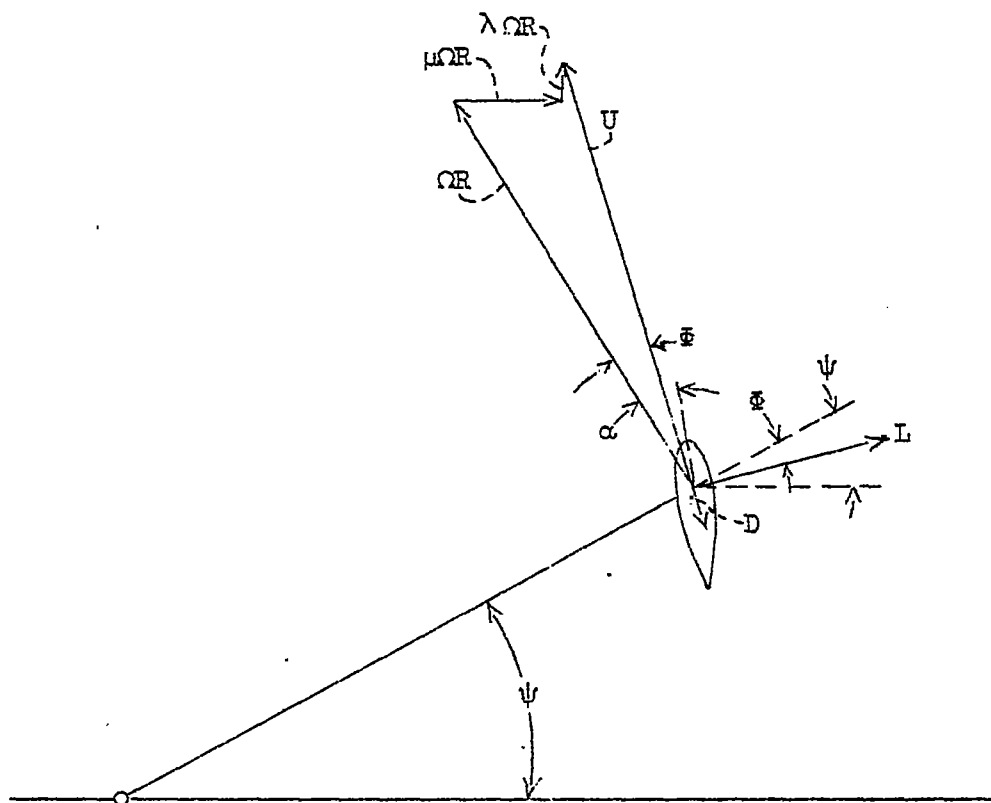


Figure 4.-Blade velocities and forces.

$$\frac{W}{2Rs} = 5 \text{ lb./sq.ft.}$$

$$A_D = 8 \text{ sq.ft.}$$

$$2Rs = 288 \text{ sq.ft.}$$

$$\theta = 0^\circ$$

$$\sigma = 0.050$$

$$\Omega R = 300 \text{ ft./sec}$$

$$C_{TA} = 0.297$$

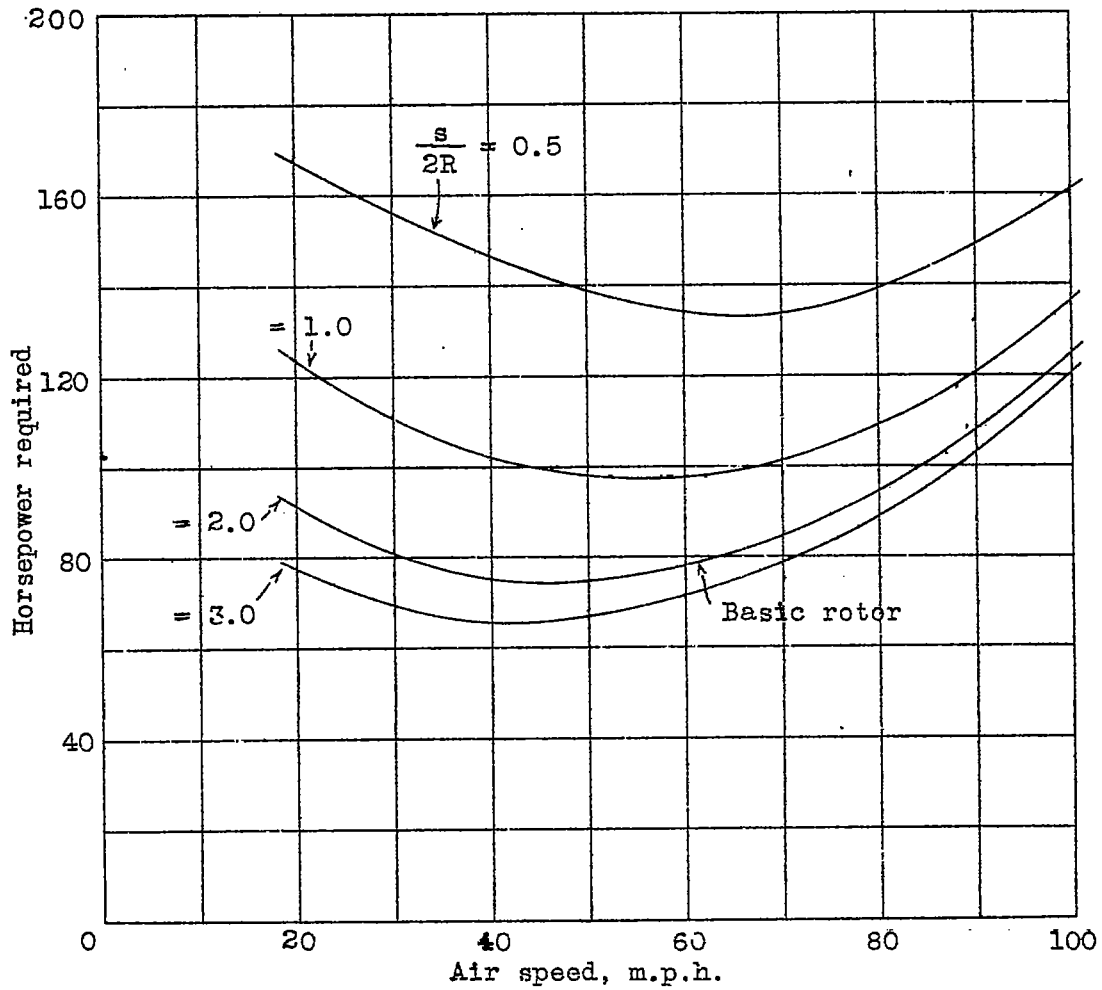


Figure 5.-Influence of span-diameter ratio on cyclogiro rotor characteristics.

$$\frac{W}{2Rs} = 5 \text{ lb./sq.ft.}$$

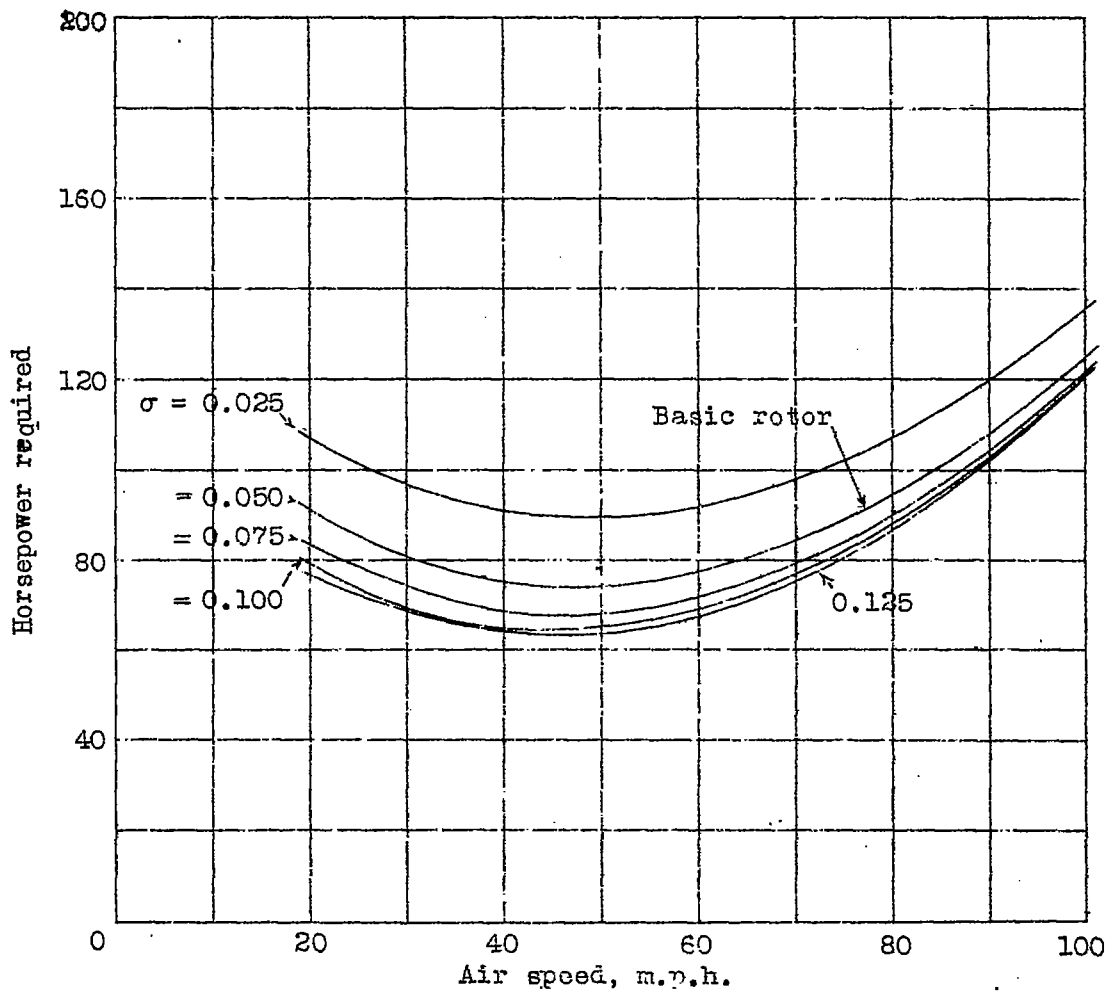
$$R = 6 \text{ ft.}$$

$$s = 24 \text{ ft.}$$

$$\theta = 0^\circ$$

$$\sigma \Omega R^2 = 4500$$

$$C_{LA} = 0.297$$



Note: ΩR varied with σ to keep C_{LA} constant.

Figure 6.-Influence of solidity on cyclogiro rotor characteristics.

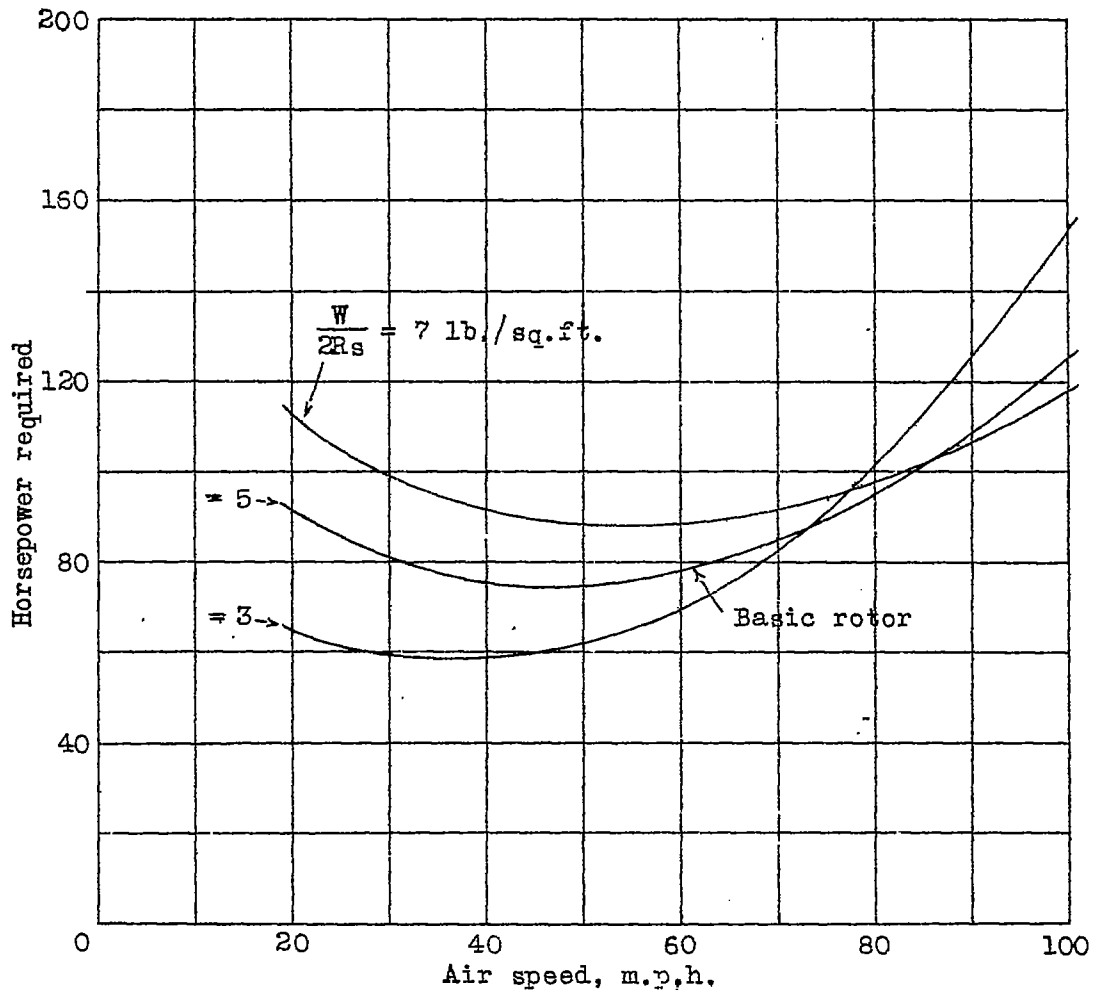
$$W = 1440 \text{ lb.}$$

$$\sigma = 0.050$$

$$\theta = 0^\circ$$

$$C_{L_A} = 0.297$$

$$\frac{s}{2R} = 2$$

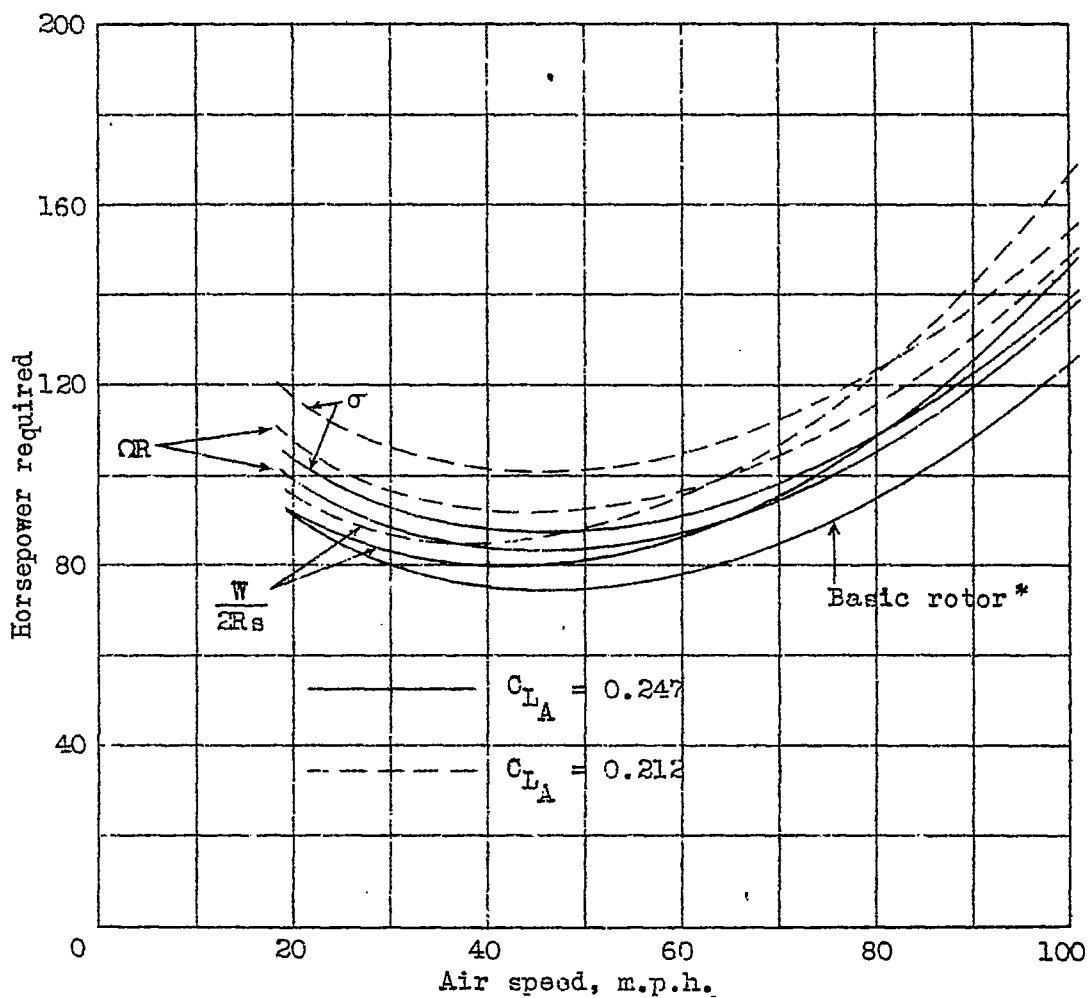


Note: CR varied to keep C_{L_A} constant. Loading varied by changing rotor size.

Figure 7.—Influence of rotor loading on cyclogiro rotor characteristics.

* $C_{L_A} = 0.297$
 $\sigma = 0.050$
 $QR = 300 \text{ ft./sec}$
 $\frac{W}{2R_s} = 5.0 \text{ lb./sq.ft.}$

$W = 1440 \text{ lb.}$
 $\frac{s}{2R} = 2$
 $A_D = 8 \text{ sq.ft.}$
 $\theta = 0^\circ$



Note: Curves are labeled to indicate parameter that has been changed to alter C_{L_A}

Figure 8.-Effect on cyclogiro rotor characteristics of varying C_{L_A} by different methods.

$2R_s = 288$ sq.ft.

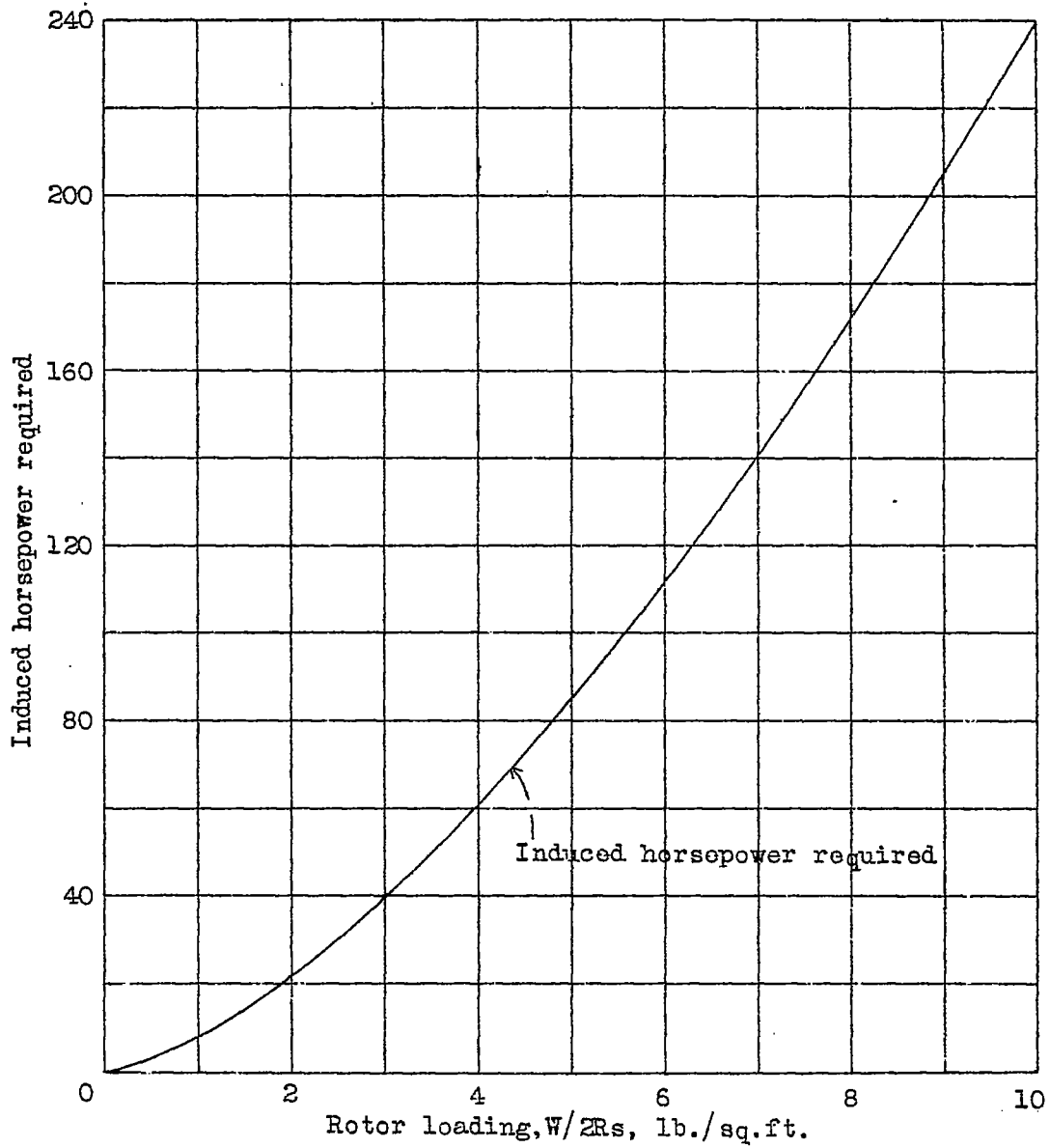


Figure 9.-Hovering flight; induced-power requirement of the cyclogiro rotor.

$2R_s = 288 \text{ sq.ft.}$
 $C_{D0} = 0.015$

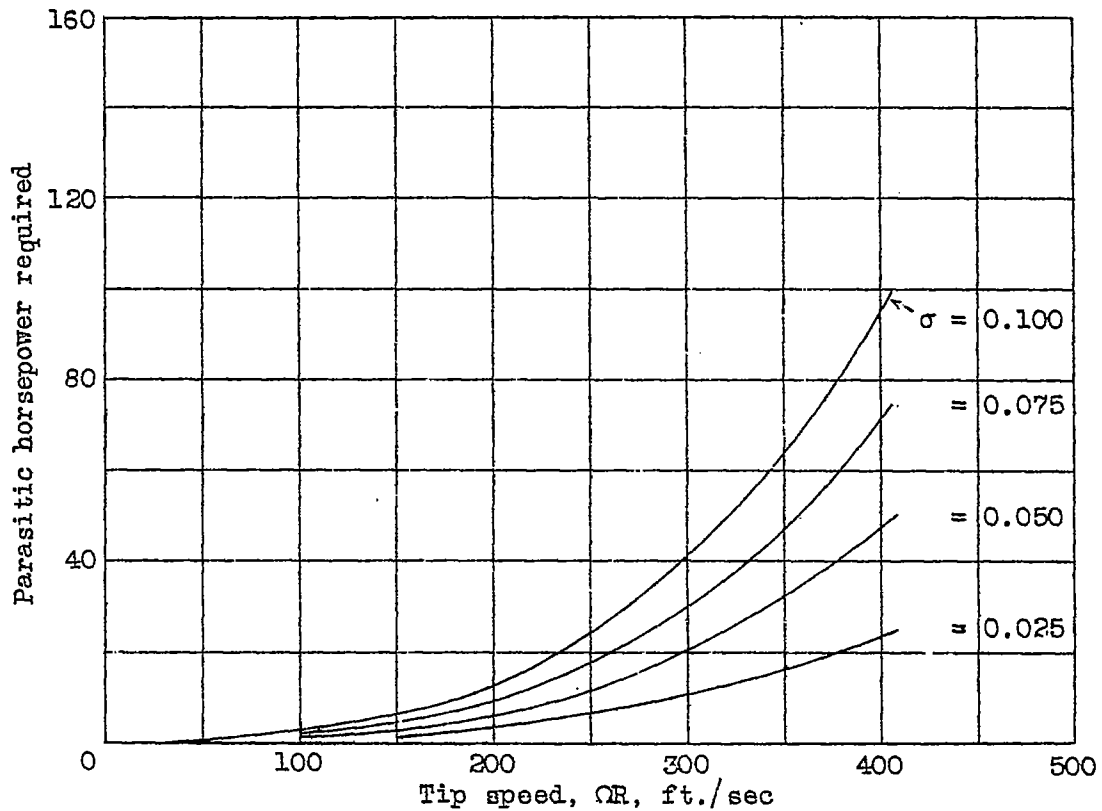


Figure 10.-Hovering flight; parasitic-power requirement of the cyclogiro rotor.

$\frac{W}{2R_s} = 5 \text{ lb./sq. ft.}$
 $\Omega R = 300 \text{ ft./sec.}$
 $\frac{s}{2R} = 2$
 $W = 1440 \text{ lb.}$
 $\sigma = 0.050$
 $a = 5.0$
 $L = 0.40$
 $\theta = 0^\circ$
 $\alpha_A = 24.8^\circ$
 $\epsilon_0 = 16.8^\circ$

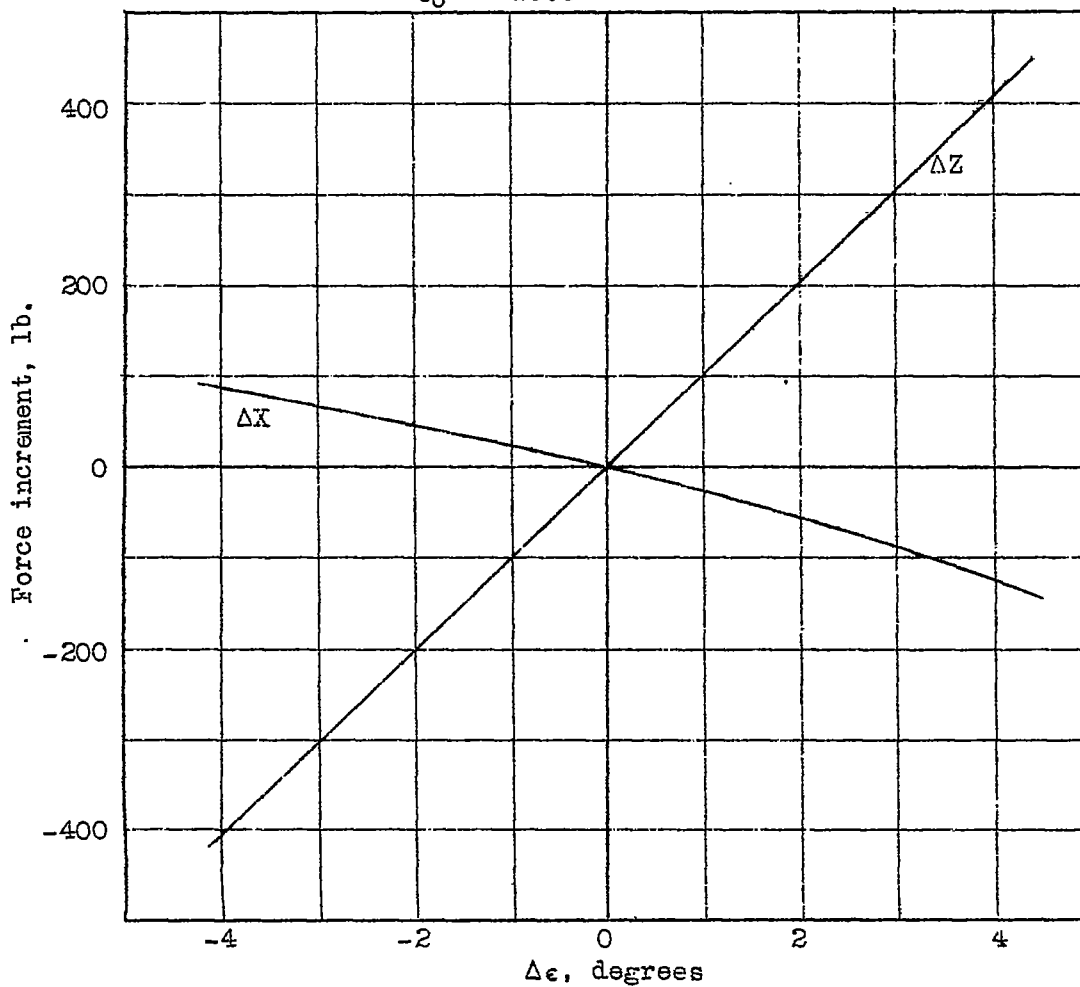
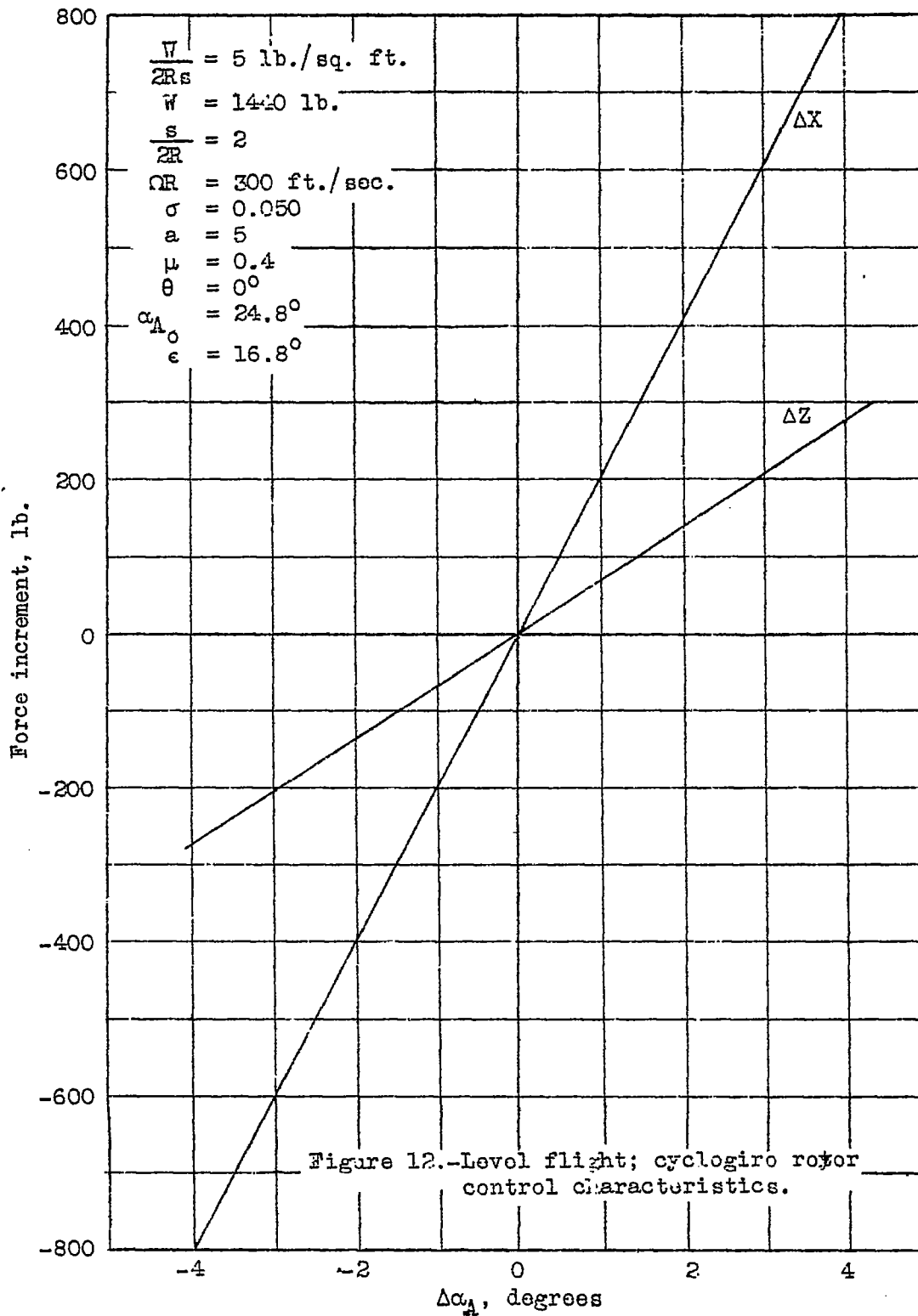
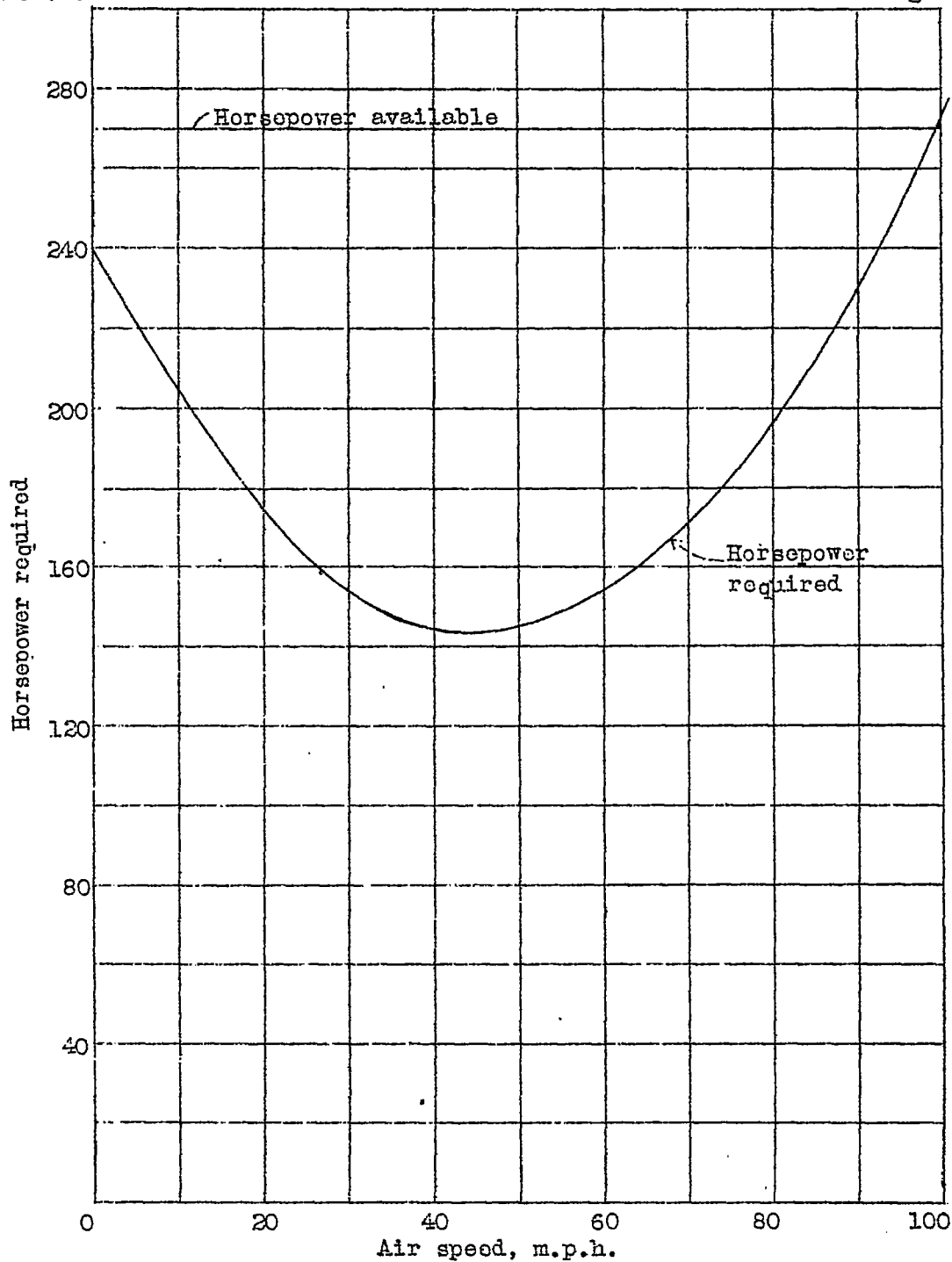


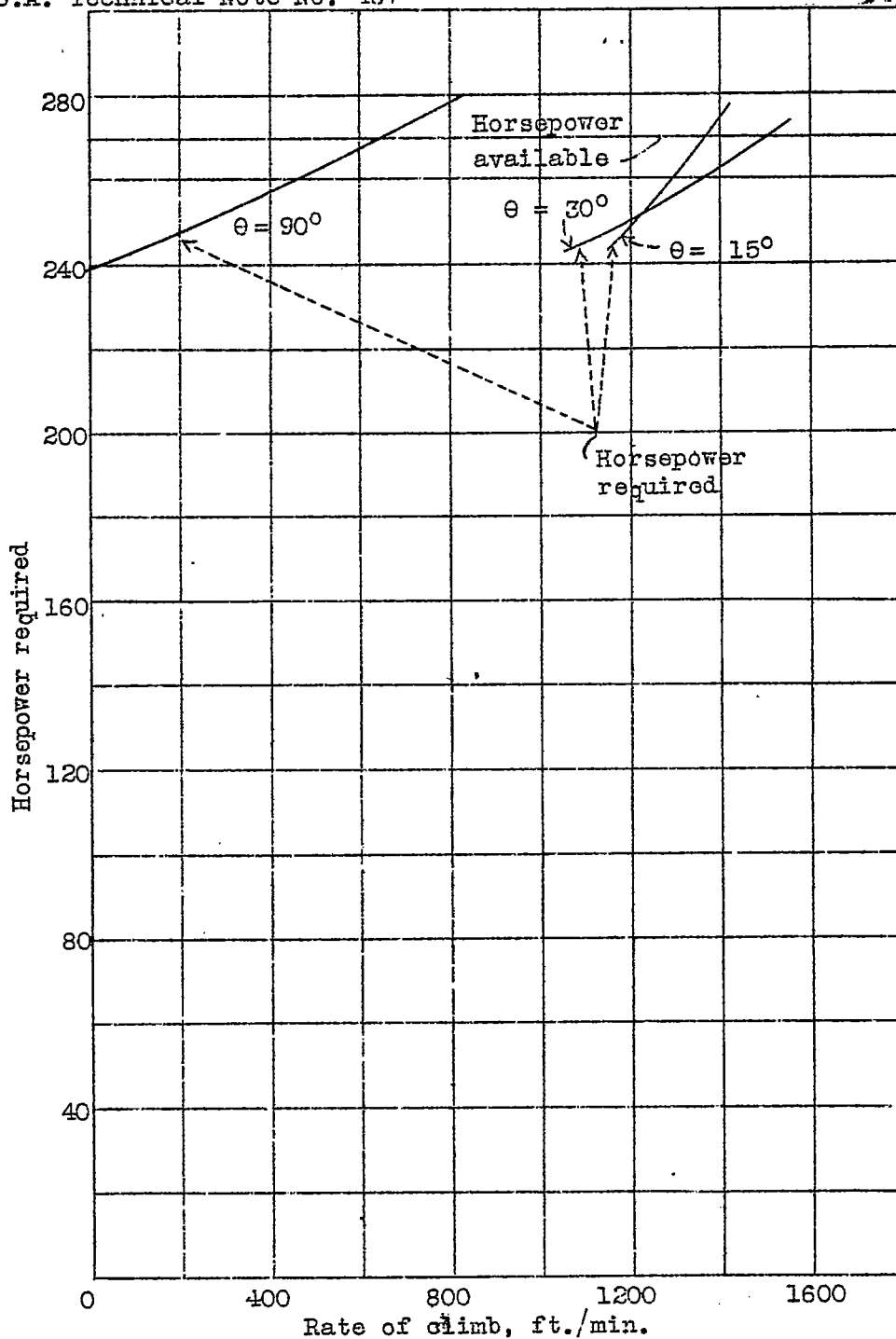
Figure 11.-Level flight; cyclogiro rotor control characteristics.





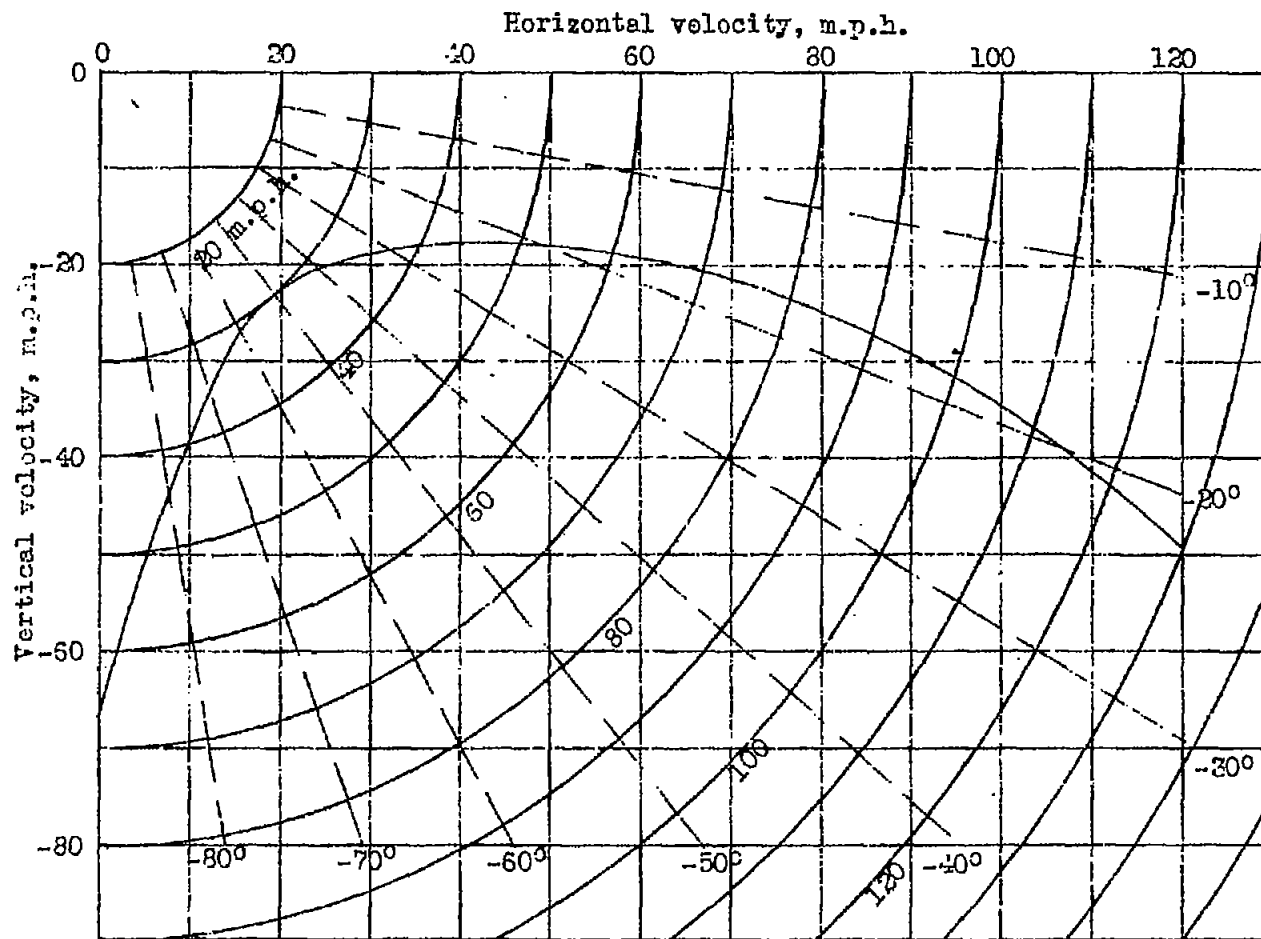
Rotor characteristics as in table II
 Brake horsepower = 300 hp
 Parasite drag area = 20 sq.ft.
 Gross weight = 3,000 lb.

Figure 13. - Level flight; cyclogiro performance.



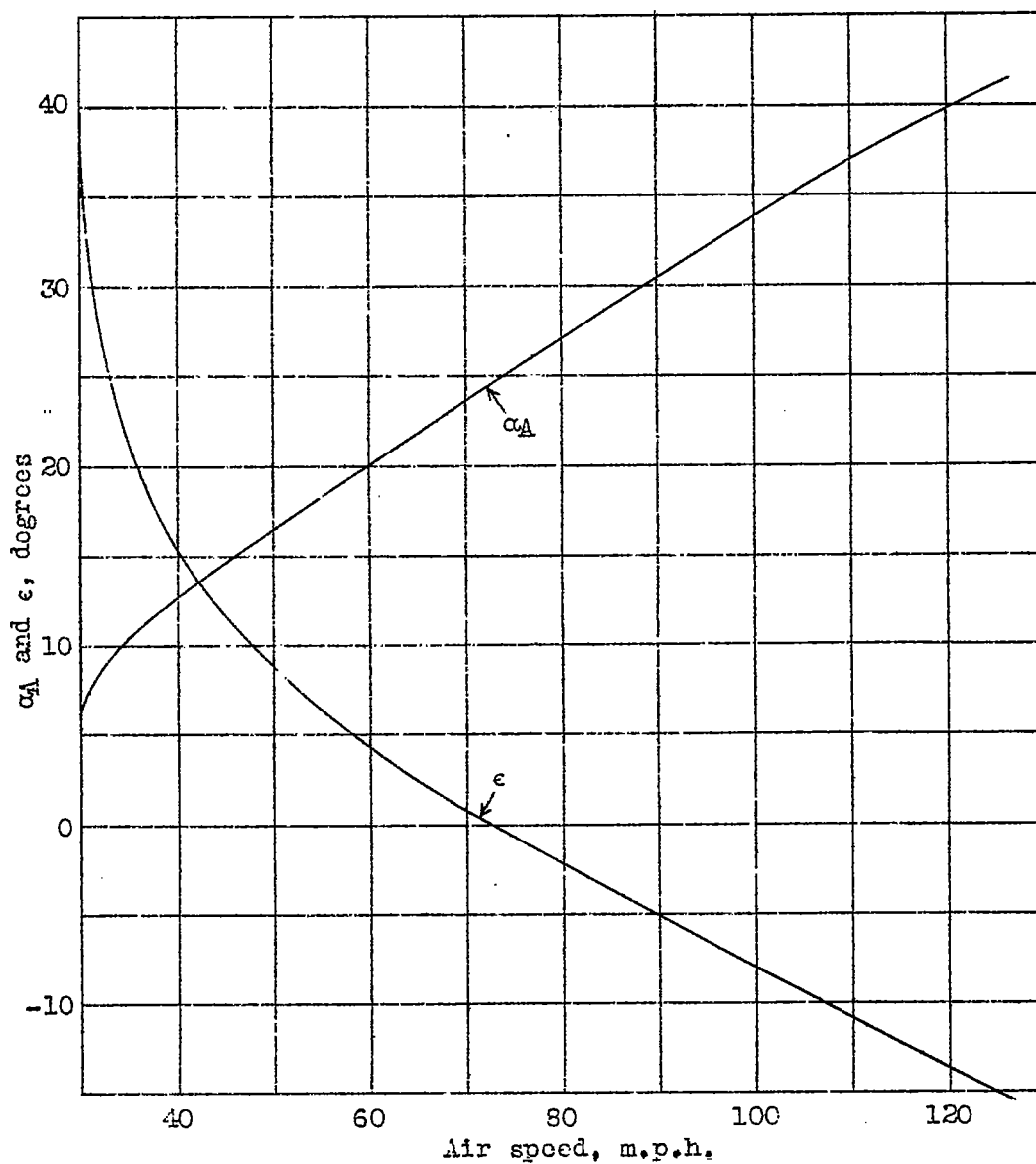
Rotor characteristics as in table II
 Brake horsepower = 300 hp
 Parasite drag area = 20 sq.ft.
 Gross weight = 3,000 lb.

Figure 14.- Cyclogiro performance, in climb.



Rotor characteristics as in table II
 Parasite drag area = 20 sq.ft.
 Gross weight = 3,000 lb.

Figure 15.- Gliding flight; cyclogiro performance.



Rotor characteristics as in table II
 Parasite drag area = 20 sq.ft.
 Gross weight = 3,000 lb.

Figure 16.- Gliding flight; cyclogiro performance; control angles required.